Reliability Analysis of Fast Electric Vehicle Charging Systems

Karunarathna, Jayani; Madawala, Udaya; Baguley, Craig; Blaabjerg, Frede; Sandelic, Monika

Published in:
2021 IEEE 12th Energy Conversion Congress & Exposition - Asia (ECCE-Asia)

DOI (link to publication from Publisher):
10.1109/ECCE-Asia49820.2021.9479384

Publication date:
2021

Document Version
Early version, also known as pre-print

Reliability Analysis of Fast Electric Vehicle Charging Systems

Jayani Karunarathna[1], Udaya Madawala[1], Craig Baguley[2], Frede Blaabjerg[3], and Monika Sandelic[3]
[1]*Department of Electrical and Computer Engineering*, *The University of Auckland*, Auckland, New Zealand
dkar412@aucklanduni.ac.nz, u.madawala@auckland.ac.nz
[2]*Department of Engineering, Computer and Mathematical Sciences*, *Auckland University of Technology*, Auckland, New Zealand
craig.baguley@aut.ac.nz
[3]*Department of Energy Technology*, *Aalborg University*, 9220 Aalborg, Denmark
fbl@et.aau.dk, mon@et.aau.dk

***Abstract*—To improve electric vehicle (EV) uptake, fast charging systems must be widely deployed. However, fast EV charging mission profiles expose power electronic components to extremely high-power stresses within short periods of time. Consequently, power electronic components in fast EV charging systems are expected to degrade/wear-out at a faster rate, requiring frequent replacement within the lifespan of the charging system. It is, therefore, important to both design and build fast EV charging systems with a known level of reliability. This paper proposes a model to investigate the reliability of fast EV charging systems. Using the model, the reliability of a typical fast EV charging system is analyzed, and results are presented to show how the lifetime and reliability of semiconductor switches used in fast EV charging systems can be predicted, even under widely varying mission profiles.**

Keywords—Mission profiles, reliability, lifetime, semiconductor switches, fast electric vehicle charging systems

I. INTRODUCTION

Electric vehicle (EV) sales around the globe have risen considerably in recent years, and this trend is expected to continue. For example, in Norway and Netherlands, the compound annual growth rate of EV sales is more than 100 % [1]. However, the limited driving range and long battery charging time are the technological barriers that currently hinder the widespread adoption of EVs. Fast (rapid) EV battery charging at high power levels is a solution to mitigate these concerns [2]. However, electronic components in fast EV charging systems are invariably subjected to higher levels of voltage and current stresses, compromising the reliability of the entire charging system. A previous study has shown that warranty/insurance and cost of maintenance are usually more expensive for fast EV chargers with components that are subjected to higher physical stress and are more vulnerable to vandalism or other physical damage [3]. The maintenance and warranty/insurance costs for fast EV chargers are estimated at $300-$3,000 per year, with an average of $2,500 per year [3]. Thus, to ensure robust operation with a low rate of failure, lifetime prediction and reliability analysis of fast EV charging systems must be performed during the design stage. Moreover, according to the industrial statistical and device manufacturer's point of view, semiconductor switches are identified as the most sensitive components to failure in a typical power electronic system [4]. Therefore, the lifetime prediction of semiconductor switches must be given the highest priority when designing reliable fast EV charging systems.

In regard to lifetime prediction, more challenging issues have to be addressed. Prior studies in estimating the lifetime of power electronic components have been typically based on statistical analysis. The MIL-HDBK-217F [5] handbook has been commonly used during this period to estimate the lifetime of power electronic components [6]. In fact, the lifetime prediction can be done in a statistical manner, specifying the reliability models of subsystems, which are typically associated with constant failure rates. Different analytical methods such as fault tree analysis [7], failure mode and effect analysis [8], Markov analysis [6], and reliability block diagram analysis [9] should then be used to estimate the reliability in a system-level point of view. Nevertheless, the models in this manual with constant failure rates are obsolete and have not been updated since 1995, leading to this manual being revoked. Another explanation for the problems associated with this method is that even though the method is simple, it is based on an assumption of constant failure rates and the impact of temperature variations is not considered [10]. Thus, the predicted reliability data using this method are difficult to apply for the development of more reliable power electronic systems.

Therefore, a conversion to a physics-of failure (PoF) focused lifetime estimation is an ongoing research topic [11], and one of the attempts of this method is to identify the root causes of power electronic failures. In prior art research [11], various failure mechanisms associated with internal material properties, physical structure, and operating conditions of power electronic systems are considered for the study of PoF based reliability estimation [11]. During the investigations, thermo-mechanical stress is observed to be one of the main causes of failures such as bond-wire damage and die-attach solder crack. The thermal stress in power electronic systems is expressed as temperature cycling, consisting of temperature fluctuations and mean temperatures. Thus, several efforts have been taken to analyze component temperatures in actual environments [12] and build strategies to maintain the temperature for improved reliability [13]. Practically, the temperature fluctuations are strongly related to the operating environments and conditions, termed to as mission profiles [14]. Therefore, reliability analysis based on the PoF method mainly involves the knowledge of mission profiles, which are time-varying inputs.

According to the literature, the reliability of power electronic systems has primarily been investigated in relation to wind and solar power applications [15, 16], and a detailed study on the reliability analysis of fast EV charging systems has not been carried-out to date. Fast EV charging is predominantly achieved through wired means and wireless fast EV charging by inductive power transfer (IPT) is still an ongoing research topic. Therefore, considering the above concerns, this paper proposes a PoF based reliability estimation model to analyze the reliability of wired fast EV

charging systems. The paper is organized as follows. The paper discusses a typical wired fast EV charging system configuration in § II. The proposed reliability estimation model is explained in § III. In § IV, a case study on a three-phase 80 kW wired fast EV charging system is presented to better demonstrate the proposed reliability estimation model under a specific mission profile. A system-level reliability analysis based on Monte Carlo simulation is provided in § IV. Finally, concluding remarks are discussed in § V.

II. Wired Fast Ev Charging

According to the United States department of energy, EV charging is classified into three main categories. Level 1 is defined as slow charging with a charging power of less than 5 kW. Level 2 is accelerated charging with a charging power between 5 kW and 50 kW. Level 3 is fast charging that is with a charging power of more than 50 kW [17]. The high charging power levels of Level 3 charging make it difficult to carry the necessary power electronic converters on-board, due to size constraints. Therefore, Level 3 charging typically transfers power to the vehicle as DC, whereas Level 1 and Level 2 charging usually have on-board electronic converters to convert AC power into DC. Because the conversion from AC to DC power takes place at the charging station in Level 3 charging, these systems can provide a higher level of power, typically 50 kW to 350 kW and above compared to the AC charging stations. A standard 50 kW DC fast charger delivers enough charge in 60 mins to provide 200 km of driving range, while a 350 kW DC fast charger only requires 10 mins to provide a 200 km range [18]. However, working with tens to hundreds of kilowatts of power, efficient conversion, reliability of the system, and user safety are critical aspects of fast EV charging systems.

In order to investigate the reliability of wired fast EV chargers, a typical three-phase wired fast EV charging system, shown in Fig. 1, was considered. The system consists of two interconnected AC/DC and DC/DC power electronic converters. The AC/DC converter draws a sinusoidal current from a three-phase AC input supply (400 V) and regulates the DC link voltage (700 V) at the output. The DC/DC converter controls the power flow required for charging the battery while providing galvanic isolation. An inner current control loop was used to control the three-phase AC/DC converter. The controller measures the phase current and controls the inductor-neutral voltage to force the phase current to follow the reference current. The value of current reference was provided by outer control loops that implement power factor control and DC voltage [19]. The DC/DC converter implementation was based on a phase-shifted dual active bridge (DAB) converter. The system input and output DC voltages are 700 V and 384 V, respectively, and the switching frequency is 100 kHz. Phase-shift modulation was used to direct the power flow in the DAB by phase-shifting the pulses of one bridge with respect to the other. According to the charging profile, an output current error signal was generated based on a current reference value. The phase shift angle for the pulse width modulation (PWM) was generated by feeding this error signal through a digital proportional integral (PI) controller. The applied square waves create a voltage differential across the energy transfer inductor and direct its stored energy. The simulation parameters used for developing this model were obtained from [20].

Using the proposed reliability estimation model presented in § III, the reliability of the two converters was analyzed from the component to the system-level, taking into account the lifetime assessments of semiconductor switches.

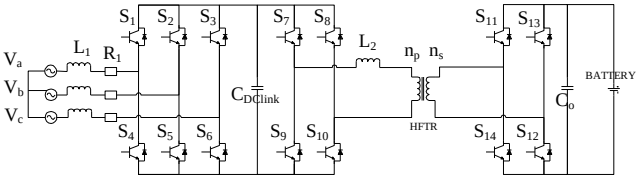

Fig. 1. A typical three-phase wired fast EV charging system.

III. Proposed Reliability Estimation Model

The proposed reliability estimation model, presented in Fig. 2., can be used to analyze the reliability of power electronic converters in the fast EV charging system shown in Fig. 1.

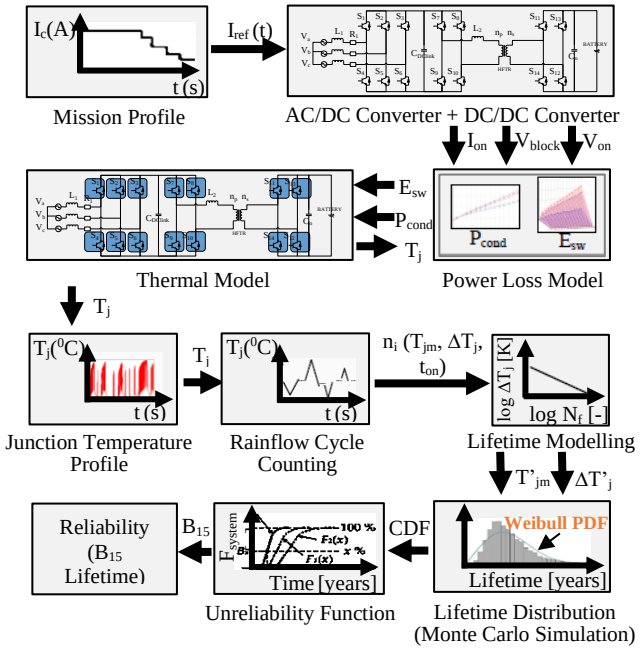

Fig. 2. Proposed reliability estimation model.

The steps in the proposed reliability estimation model can be summarized as:

- Mission profile interpretation
- Thermal modelling of semiconductor switches
- Rainflow cycle counting method
- Lifetime modelling
- Lifetime distribution
- System-level reliability analysis

which will be explained in details in the following sections.

A. Mission Profile Interpretation

The operating conditions of the power electronic converter throughout the operation must be known in order to estimate the reliability [11]. In this regard, a mission profile, which is related to the operating conditions of the power electronic system, is required. Hence, in this study, the charging profile of the fast EV charging system was considered as the mission profile, since it directly relates to the operating conditions of the fast EV charger. Moreover, multistage constant current (MSCC) charging profile is the most common charging profile used for fast EV charging. Thus, the MSCC charging profile

was used. Different stages of current values in the MSCC charging profile were considered as the current reference values and, applied as the inputs to the current controller in the DC/DC converter. In order to implement the optimal charging pattern of currents in the MSCC profile, the method proposed in [21] was used. The MSCC profile was implemented with five stages of optimized current values, which give the minimum charge time. The current values in each stage were applied to the battery until the battery voltage reaches a predetermined maximum allowable value.

B. Thermal Modelling of IGBT Power Modules

Since junction temperature is the main life-limiting factor in semiconductor switches resulting in a bond wire lift-off [22], the above mission profile must be converted into junction temperature variations of the semiconductor switches. Once the charging mission profile is applied to the fast charging system, the power losses in the semiconductor switches can be calculated. These power losses are usually calculated using the look-up table (LUT) approach, in the PLECS simulator. Thus, the power losses are obtained in advance for a specific set of operating conditions. Then LUT can be used to interpolate the power losses under the required operating conditions. The junction temperature variation due to power losses can be obtained using the thermal model of the semiconductor switches, which is usually given in the device's datasheet.

C. Rainflow Cycle Counting Method

By following the aforementioned method, the junction temperatures of the semiconductor switches under a particular mission profile can be determined. Usually, because of the dynamics of the mission profile, the junction temperature has an irregular pattern. Therefore, a cycle counting method, such as Rainflow cycle counting, is performed to identify the regular thermal cycles within the irregular cycles in the junction temperature profile [23]. In this manner, relevant data such as the temperature cycle amplitude (ΔT_j), the mean junction temperature (Tjm), and the cycle period (t_{on}) can be determined and applied directly to the lifetime model.

D. Lifetime Modelling

The power cycling capability of semiconductor switches is modelled by a Coffin-Manson law, where the number of cycles to failure is assumed to be proportional to the junction temperature cycle amplitude [5]. According to [24], a standard lifetime model of a semiconductor switch can be given as:

$$N_f = A \times (\Delta T_j)^{\alpha} \times (ar)^{\beta_1 \Delta T_j + \beta_0} \times \left[\frac{C + (t_{on})^{\gamma}}{C+1}\right] \times exp\left(\frac{E_a}{k_b \times T_{jm}}\right) \times f_d \quad (1)$$

where N_f is the number of cycles to failure. The input data of this lifetime model are T_{jm}, ΔT_j, and t_{on}, which are obtained from the Rainflow cycle counting method. The rest of the parameters can be found in [24]. Usually, the lifetime of the power electronic components is expressed in terms of life consumption (LC). The LC value implies how much life of the component has been damaged or consumed during the operation. The Palmgren Miner's rule can be used to determine the LC [25] as:

$$\mathrm{LC} = \sum_{\mathrm{i}} \frac{n_i}{N_{fi}} \quad (2)$$

where n_i is the number of cycles for a particular T_{jm}, ΔT_j, and t_{on}. The power electronic component is considered to reach its end of life when its LC accumulates to unity.

E. Lifetime Distribution

The lifetime predictions of the semiconductor switches obtained from (2) can be considered as an ideal case, where the time to failure of all of the components is same. However, in practice, components don't fail at the same rate, due to stress changes, variations in the lifetime model parameters, and manufacturing variations. Thus, it is appropriate to present the lifetime predictions in terms of a statistical value, instead of a fixed value. To accomplish this, it is necessary to carry out the Monte Carlo analysis [26]. The Monte Carlo method introduces changes in the lifetime model parameters and determines the lifetime with significant sample size. Then the results will merge to the required value, with a large enough sample size. In this approach, all the parameters in the lifetime model in (2) must be modelled by a probability distribution function introducing a particular variation range. Applying the Monte Carlo simulation, a particular number of samples from each parameter distribution are selected at random to determine the lifetime of the semiconductor switches. Thus, a set of lifetime prediction results are obtained. In general, lifetime data of the semiconductor switches follow a Weibull distribution [27]. The probability density function (PDF) of the Weibull distribution is typically considered as a lifetime distribution $f(x)$, while its cumulative distribution function (CDF) is acknowledged as an unreliability function $F(x)$. Usually, the reliability is represented by B_{15} lifetime, which is the time taken for 15% of the population to fail [28]. Thus, by considering the unreliability function, the reliability or the B_{15} lifetime of the semiconductor switch can be obtained.

F. System-Level Reliability Analysis

In many instances, power electronic converters are made up of several semiconductor switches, each with its specific unreliability function $F(x)$. Therefore, the reliability block diagram of the complete system must be developed in order to evaluate the reliability in system-level [29]. The reliability block diagram illustrates how the reliability of components in the system relates to one another. If a system consists of n number of components and the system fails to operate if any of the components fails, the overall unreliability function of the system $F_{\mathrm{tot}}(x)$ can be evaluated as:

$$F_{\mathrm{tot}}(x) = 1 - \prod_{\mathrm{n}=1}^{\mathrm{n}} (1 - F_{\mathrm{n}}(x)) \quad (3)$$

where $F_{\mathrm{n}}(x)$ is the unreliability function of the n^{th} component. After obtaining the overall unreliability function of the converter system $F_{\mathrm{tot}}(x)$, by following the same method used for a single semiconductor switch, the B_{15} lifetime of the complete converter system can be determined. This concept is applicable to any power electronic system. The reliability block diagram of the system can vary according to the number of components and the operating principles for different converter topologies.

IV. Case Study

A. Mission Profile of the Case Study

The thermal behaviours of the semiconductor switches in the converters shown in Fig. 1 were first observed by feeding a MSCC charging load, shown in Fig. 3, for a charging period

of 1325 s. The five stages of currents in the charging profile and the charging period were obtained according to the method described in § III.A. The current values in each stage were applied to the battery until the battery voltage reaches a predetermined maximum allowable value of 384 V.

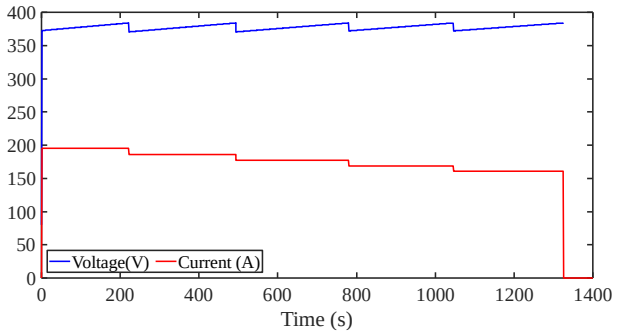

Fig. 3. Fast EV charging profile.

B. Thermal Loading

Applying the mission profile translation method described in § III.B, the junction temperatures of the semiconductor switches were obtained. The junction temperature profiles of a single semiconductor switch in the AC/DC converter and DC/DC converter are depicted in Fig. 4 and Fig. 5, respectively. It can be observed that the junction temperature of the switch reaches its highest value at 90 ^{0}C in the AC/DC converter and 107 ^{0}C in the DC/DC converter, while its minimum value is 25 ^{0}C in both converters.

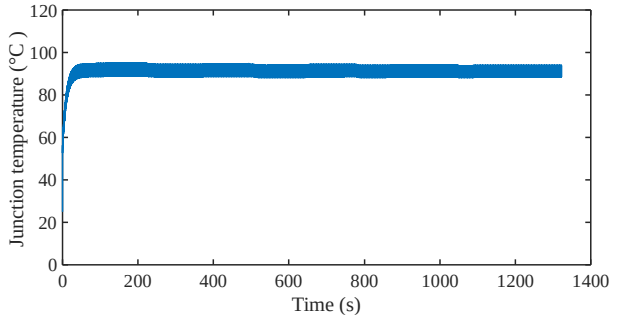

Fig. 4. Junction temperature profile of a single semiconductor switch in the AC/DC converter.

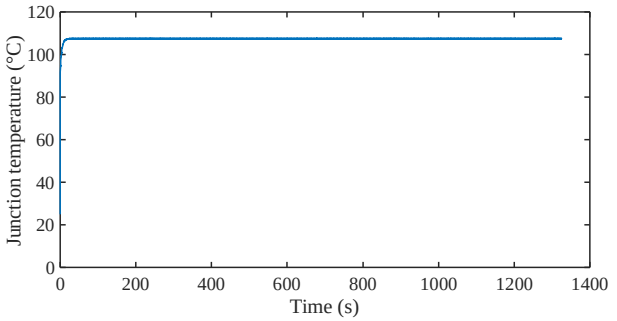

Fig. 5. Junction temperature profile of a single semiconductor switch in the DC/DC converter.

C. Translated Thermal Loading with Cycle Counting

The Rainflow matrix histograms for the junction temperatures of the semiconductor switches are shown in Fig. 6. The majority of the temperature cycles have a T_{jm} value of 90 ^{0}C with a ΔT_j of about 3 ^{0}C in the case of AC/DC converter and a T_{jm} value of 107 ^{0}C with a ΔT_j of about 1 ^{0}C in the case of DC/DC converter.

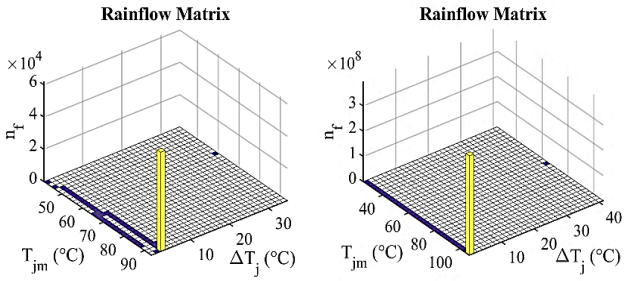

Fig. 6. Rainflow matrix for the junction temperature in the AC/DC converter switch (left) and DC/DC converter switch.

D. Lifetime Evaluation

The results of Rainflow cycle counting were applied to the lifetime model in (1) in order to determine the LC of a semiconductor switch. The resultant LC for a single semiconductor switch in the three-phase AC/DC converter is 0.0256/year. This implies that the semiconductor switch is expected to reach its end of useful life after 39 years of operation. Furthermore, the LC for a single semiconductor switch in the DC/DC converter is 0.0533/year. This implies that the semiconductor switch is expected to reach its end of useful life after 19 years of operation.

Moreover, the Monte Carlo simulation was performed to evaluate the lifetime by taking into account parameter uncertainties in the lifetime model. Thus, a normal distribution with a 5% parameter variation was applied to introduce the parameter variations to the parameters of the lifetime model described in (1). The inputs of the lifetime model, which are stress parameters, T_{jm}, ΔT_j, and t_{on}, should also be modelled by a normal distribution function introducing a 5% parameter variation. In order to do so, the equivalent static values of these dynamic parameters, which dynamically vary throughout the operations, must be calculated. The equivalent static values of the stress parameters are the representative values of the thermal stresses, which result in the same LC. The line frequency of 50 Hz thermal cycling was considered for the AC/DC converter. Thus, the equivalent number of cycles per year (n'_i) was (365×24×60×60)×50 cycles, and the equivalent cycle period (t'_{on}) was selected to be 0.01 ms. On the other hand, the switching frequency of 100 kHz thermal cycling was considered for the DC/DC converter and the n'_i was (365×24×60×60)×100×10^3 cycles, and the t'_{on} was selected to be 0.005 ms. The equivalent mean junction temperature (T'_{jm}) was obtained by averaging the junction temperature profiles in Fig. 4 and Fig. 5. Then, the equivalent static value of cycle amplitude ($\Delta T'_j$) was determined using (1).

The obtained equivalent static values were also modelled with a normal distribution function, using the same method applied previously for the modelling of lifetime model parameters. Afterwards, the Monte Carlo simulation was performed with a population of 10000 samples, in order to obtain the LC and the respective lifetime for 10000 samples. In fact, the semiconductor switch's lifetime distribution $f(x)$, can be represented by a Weibull distribution [30] with a PDF described as:

$$f(x) = \frac{\beta}{\eta^{\beta}} x^{\beta-1} \exp\left[-\left(\frac{x}{\eta}\right)^{\beta}\right] \qquad (4)$$

where η is the scale parameter and β is the shape parameter. The value of η corresponds to the time when 63.2% of the population has failed, while the value of β usually indicates a failure mode [30]. After obtaining the lifetime distributions $f(x)$ and corresponding Weibull PDFs of the semiconductor switches, the unreliability functions were obtained as described in § III.E. The obtained unreliability functions using the Monte Carlo simulation for 10000 samples are shown in Fig. 7 and Fig. 8. As evident, the reliability, represented by B_{15} lifetime of one single semiconductor switch in the AC/DC converter, is 25 years. This indicates that 15% of the population is expected to fail after 25 years. Moreover, the reliability of one single semiconductor switch in the DC/DC converter is 10 years, which indicates that 15% of the population is expected to fail after 10 years.

E. System-Level Reliability Analysis of the Case Study

The reliability block diagram was used to evaluate the reliability in system-level based on the component-level unreliability functions F(x) obtained from the Monte Carlo simulation. The three-phase AC/DC converter consists of six semiconductor switches and the converter cannot function if any of the switches fails. Similarly, the DC/DC converter consists of eight semiconductor switches and the converter cannot function if any of the switches fails. Furthermore, in both converters, the loading of each semiconductor switch is equal. Therefore, each switch has the same unreliability function. Thus, the system-level unreliability functions of the AC/DC converter and DC/DC converter can be determined as:

$$F_{\text{tot, AC/DC}}(x) = 1 - \left(1 - F(x)\right)^6 \tag{7}$$

$$F_{\text{tot, DC/DC}}(x) = 1 - \left(1 - F(x)\right)^8 \tag{8}$$

The system-level unreliability functions of the converters are presented in Fig. 7 and Fig. 8, together with the corresponding system-level B_{15} lifetimes.

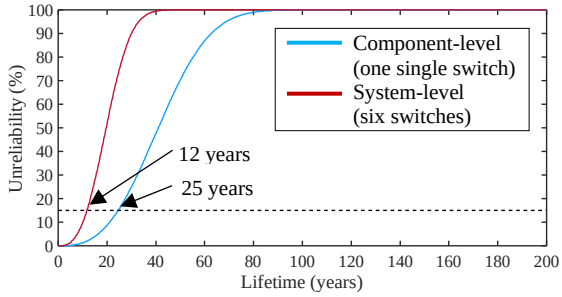

Fig. 7. Component-level and system-level unreliability functions of the AC/DC converter.

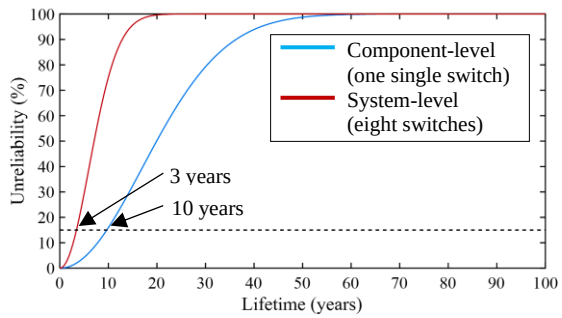

Fig. 8. Component-level and system-level unreliability functions of the DC/DC converter.

The system-level B_{15} lifetime or the reliability of the AC/DC converter is 12 years, which is 13 years lower than the component-level B_{15} lifetime. Moreover, the system-level B_{15} lifetime or the reliability of the DC/DC converter is 3 years, which is 7 years lower than the component-level B_{15} lifetime. Furthermore, by introducing rest periods after each charging, lifetime prediction results can be obtained with improved reliability.

V. Conclusion

To implement robust fast EV charging systems, a reliability estimation model has been presented in this paper. Comprehensive mathematical and simulation models have been developed to analyze voltage, current, and thermal stresses on semiconductor switches used in a wired fast EV charging system subjected to a given mission profile. A reliability estimation model has been proposed to predict the lifetime and analyze the reliability as a function of thermal cycling information. Using the proposed model, the reliability of a typical wired fast EV charging system has been analyzed, by considering the lifetime assessments of semiconductor switches. Such reliability information obtained through the proposed reliability estimation model can be used in the design stage of fast EV charging systems.

References

[1] "Evolution electric vehicles in Europe: gearing up for a new phase?", Mc Kinsey & Co, 2016.

[2] M. Yilmaz and P. T. Krein, "Review of battery charger topologies, charging power levels, and infrastructure for plug-in electric and hybrid vehicles," IEEE Trans. Power Electron., vol. 28, no. 5, May 2013.

[3] H. Lee and A. Clark, "Charging the future: Challenges and opportunities for electric vehicle adoption," Faculty Research Working Paper Series, Harvard Kennedy School, pp. 33-34, Sep 2018.

[4] Y. Song and B. Wang, "Survey on reliability of power electronic systems," IEEE Trans. Power Electron., vol. 28, pp. 591-604, 2013.

[5] U.S. Department of Defense, "MIL-HDBK-217F – Military handbook for reliability prediction of electronic equipment," Department of Defense, Washington DC, USA, Dec 1991.

[6] S. V. Dhople, A. Davoudi, A. D. Dominguez-Garc ia, and P. L. Chapman, "A unified approach to reliability assessment of multiphase dc-dc converters in photovoltaic energy conversion systems IEEE Trans. Power Electron., vol. 27, no. 2, pp. 739–751, Feb 2012.

[7] G. R. Biswal, R. P. Maheshwari, and M. L. Dewal, "Cool the generators: System reliability and fault tree analysis of hydrogen cooling systems," IEEE Ind. Electron. Mag., vol. 7, no. 1, pp. 30–40, Mar 2013.

[8] S. Haghbin, "Electrical failure mode and effect analysis of a 3.3 kW onboard vehicle battery charger," in Proc. EPE - ECCE Europe, pp. 1-10, Sep 2016.

[9] M. Cepin, "Reliability block diagram in assessment of power system reliability," Springer, pp. 119–123, 2011.

[10] B. Burger and D. Kranzer, "Extreme high efficiency PV-power converters," in Proc. EPE - ECCE Europe, pp. 1–13, Sep 2009.

[11] H. S. H. Chung, H. Wang, F. Blaabjerg, and M. Pechut, "Reliability of power electronic converter systems," IET, 2015.

[12] H. Luo, Y. Chen, P. Sun, W. Li, and X. He, "Junction temperature extraction approach with turn-off delay time for high-voltage high-power IGBT modules," IEEE Trans. Power Electron., vol. 31, no. 7, pp. 5122-5132, Jul 2016.

[13] K. Ma, M. Liserre, and F. Blaabjerg, "Reactive power influence on the thermal cycling of multi-MW wind power inverter," IEEE Trans. Ind. Appl., vol. 49, no. 2, pp. 922–930, Mar 2013.

[14] Y. Yang, H. Wang, F. Blaabjerg, and K. Ma, "Mission profile based multi-disciplinary analysis of power modules in single-phase transformerless photovoltaic inverters," in Proc. EPE – ECCE Europe, pp. 1–10, Sep 2013.

[15] W. Huai, M. Ke, and F. Blaabjerg, "Design for reliability of power electronic systems," IEEE Ind. Electron., pp. 33-44, 2012.

[16] J. Rocabert, A. Luna, F. Blaabjerg and P. Rodriguez, “Control of power converters in AC microgrids,” IEEE Trans. Power Electron., vol. 27, pp. 4734-4749, 2012.

[17] Department of Energy, “Vehicle Charging,” Available online: https://www.energy.gov/eere/electricvehicles/vehicle-charging (accessed on 13 February 2019).

[18] S. Bai and S. M. Lukic, “Unified active filter and energy storage system for an MW electric vehicle charging station,” IEEE Trans. Power Electron., vol. 12, 5793–5803, 2012.

[19] E. Wang and S. Huang, “A control strategy of three phase voltage sourced PWM rectifier,” International Conference on Electrical Machines and Systems, 2011.

[20] George and Kenny, “Design and control of a bidirectional dual active bridge DC-DC converter to interface solar, battery storage, and grid-tied inverters”, Electrical Engineering Undergraduate Honors Thesis, 2015.

[21] A. B. Khan and W. Choi, “Optimal charge pattern for the high-performance multistage constant current charge method for the li-ion batteries,” IEEE Trans. Energy Conversion, vol. 33, no. 3, Sep 2018.

[22] V. Smet, F. Forest, J. J. Huselstein, F. Richardeau, Z. Khatir, S. Lefebvre, and M. Berkani, “Ageing and failure modes of IGBT modules in high temperature power cycling,” IEEE Trans. Ind. Electron, vol. 58, no. 10, pp. 4931–4941, Oct 2011.

[23] H. Huang and P. A. Mawby, “A lifetime estimation technique for voltage source inverters,” IEEE Trans. Power Electron., vol. 28, no. 8, pp. 4113–4119, Aug 2013.

[24] B. Burger and D. Kranzer, “Extreme high efficiency PV-power converters,” in Proc. EPE - ECCE Europe, pp. 1–13, Sep 2009.

[25] Y. Furusho and K. Fujii, “1-MW solar power conditioning system with boost converter using all-SiC power module,” in Proc. CIPS, pp. 1-5, Mar 2016.

[26] P. D. Reigosa, H. Wang, Y. Yang, and F. Blaabjerg, “Prediction of bond wire fatigue of IGBTs in a PV inverter under a long-term operation,” IEEE Trans. Power Electron., vol. 31, no. 10, pp. 7171–7182, Oct 2016.

[27] ZVEI - German Electrical and Electronic Manufacturers’ Association, “How to measure lifetime for robustness validation - step by step,” Rev. 1.9, Nov 2012.

[28] M. Sandelic, A. Sangwongwanich and F. Blaabjerg, “Reliability evaluation of PV systems with integrated battery energy storage systems: DC-coupled and AC-coupled configurations,” Electron., no. 8, pp. 1059, 2019.

[29] Y. Song and B. Wang, “Survey on reliability of power electronic systems,” IEEE Trans. Power Electron., vol. 28, no. 1, pp. 591-604, Jan 2013.

[30] L. M. Moore and H. N. Post, “Five years of operating experience at a large, utility-scale photovoltaic generating plant,” Prog. Photovolt: Res. Appl., vol. 16, no. 3, pp. 249-259, 2008.